

## Effects of In-Situ Mechanical and Chemical Polishing on Surface Topography of Additively Manufactured Fiber-Reinforced Polymers

Aman Nigam, Bruce L. Tai

Department of Mechanical Engineering

Texas A&M University, College Station, TX 77843, USA

### Abstract

Additive manufacturing of fiber-reinforced polymers (FRPs) has revolutionized fused filament fabrication (FFF) by producing polymeric parts with enhanced mechanical properties. However, FFF suffers from poor surface quality and dimensional accuracy, particularly for FRPs, due to their abrasive and rheological nature. This examines an in-situ polishing scheme for FRPs in the FFF configuration. Glass-fiber-reinforced Nylon was used as the study material. Three polishing schemes, mechanical, chemical, and a combined thereof, were adopted along with various parameters in each case. The results show significant surface improvements in all cases, and the combined process can further reduce the Ra value to around 2  $\mu\text{m}$  and the dimensional error to 0.2 mm and less. The combined process also enhances surface uniformity (i.e., similar Ra in all directions). In particular, with the combined approach, the in-situ polishing scheme is expected to improve the quality of 3D printed FRPs significantly.

Keywords: Fiber-reinforced polymer, Fused Filament Fabrication (FFF), Hybrid process, Polishing, 3D Printing, Surface roughness.

### 1. Introduction

In recent times, polymer and polymer composites have drawn significant attention in manufacturing owing to their excellent mechanical, physical, and thermal properties. Fiber-reinforced polymers (FRPs) are characterized by properties such as high strength to weight ratio, high modulus, high fracture toughness, corrosion, and thermal resistance [1]. Due to these advantageous properties, FRPs have become a cost-effective alternative to traditional metals in aerospace, marine, oil and gas, and process industries [2]. Hand lay-up is the most popular and widely used open-mold, fiber composite manufacturing technique. However, the production rates are low, and both material and labor costs are high [3]. Further, finishing processes that involve machining and trimming are often required and essential to meet the design requirements [4]. As the application field of FRPs expands, the opportunity for improving and modifying the current manufacturing techniques has increased for its fabrication.

The last decade witnessed an exponential development in additive manufacturing, and it continues to grow due to its economic and versatile nature. The use of FRPs has transformed additive manufacturing into a robust technique and has enabled the prototyping of highly customized parts with enhanced properties. The solid model is sliced into individual layers in this automated manufacturing method, which gets printed in a stacked fashion. FRPs can be additively manufactured by fused filament fabrication (FFF) with either short (chopped) or continuous fiber configurations. Although continuous fiber configuration offers excellent mechanical properties in

certain directions, the major drawbacks include the lack of design flexibility and supplier-defined cloud-based slicing software [5]. In comparison, short-fiber printing remains the most popular and versatile approach in the additive manufacturing of FRPs.

The surface quality of FFF manufactured parts is typically poor and depends on the layer resolution and material properties [6]. This drawback of FFF, when coupled with the abrasive nature of FRPs, leads to inferior surface topography [7]. Conventional machining methods such as milling are typically used to enhance the surface finish of these materials. However, due to the abrasive and anisotropic nature of FRPs, machining of such materials often fail by matrix cracking, fiber pull-out, swelling, and delamination [8]. Kuram studied the micro-machinability of polyamide 6 (Nylon), and glass-fiber reinforced polyamide 6 manufactured by injection molding. Tool wear, cutting forces, and surface roughness were evaluated at different spindle speeds and feed rates. It was concluded that forces increased with feed rate and spindle speed, but surface roughness decreased with spindle speed for both workpiece materials. It was also pointed out that the friction between the tool and the workpiece material can induce heat generation at the contact area, leading to the softening of the polymer, thus impairing surface quality [9]. Further, Parandoush et al. examined the mechanical finishing process for 3D printed carbon fiber reinforced polymers composites via CNC milling. The surface roughness of original and finished samples was compared at various cutting depths. A 70% reduction in Ra was reported with a smooth, consistent, and predictable surface morphology after finishing [10]. These studies were successful to a certain extent; however, the post-processing requires multiple machines to fabricate and polish, making them expensive, time-consuming, and less flexible. Also, manual finishing of these FRPs results in health-related issues due to the harmful dust formation [11,12].

In addition to improving the surface finish by mechanical means, extensive work has also been published in the chemical polishing of 3D printed polymers, but not specifically for FRPs. Most of the studies were carried out either by immersing the printed part in a suitable chemical solvent or introducing it in a vapor environment in hot or cold conditions [13,14]. The solvent erodes the surface's polymer material, and the surface tension forces drive a reduction in the surface roughness. Kuo et al. developed a device to chemically polish ABS printed parts using acetone vapors. The surface finish improvement was found to be more than 88%, and similar results were observed for parts with different curvatures [15]. Nigam et al. presented a novel concept of in-process mechanical and chemical polishing of fused filament fabrication (FFF) and examined its feasibility in improving surface finish and dimensional accuracy. More than an 85% reduction in surface roughness was observed with significantly reduced form errors for ABS [16]. While the results from these investigations are vital in reducing the surface roughness, they are primarily limited to simple polymers such as ABS. No or very limited work has been reported for more functional, fiber-reinforced polymer composites.

Henceforth, considering the limitations of past research and challenges of finishing additively manufactured FRPs, this study aims to examine the effects of mechanical, chemical, and combined polishing of FRPs in an in-situ additive manufacturing environment. A custom three-axis hybrid manufacturing setup was built to provide precise motion control and repeatability of polishing parameters. A glass fiber-reinforced polymer (GFRP) in short fiber configuration was

used, and a factorial analysis was conducted to quantify the effects of spindle speed, feed rate, chemical polishing depth, and speed on surface roughness and dimensional accuracy. Further, statistical analysis was conducted to determine the optimum parameters in individual polishing schemes to design a combined mechanical plus chemical polishing approach.

To structure this paper, the experimental setup, methods, and analysis techniques are explained in Section 2. Section 3 enlists and discusses the results obtained after experiments for multiple cases. Finally, section 4 draws the concluding remarks and the future scope of this research.

## 2. Experimental Setup and Testing Methodology

### 2.1 Setup and Test Specimen

To fulfill the objectives of this research, it was essential to conduct polishing in a precise and repeatable manner. Experiments were carried out using the setup shown in Fig.1. A hybrid manufacturing setup with simultaneous printing and polishing capabilities was built, integrated with a servo-assisted motion control system (Moog Animatics, USA). A high-speed spindle (NSK, Japan) with a carbide end mill (3.175 mm diameter, three flutes) was employed for mechanical polishing at different spindle speeds. Additionally, a pen-style device filled with a suitable chemical solvent (formic acid for nylon-6) was used for chemical polishing. This device was connected to a reservoir with a flow control valve to regulate the rate of chemical dispensing to ensure a controlled erosion process. This method controls both the solvent dispensing rate and the normal force applied on the surface. More details are discussed in the subsequent sections.

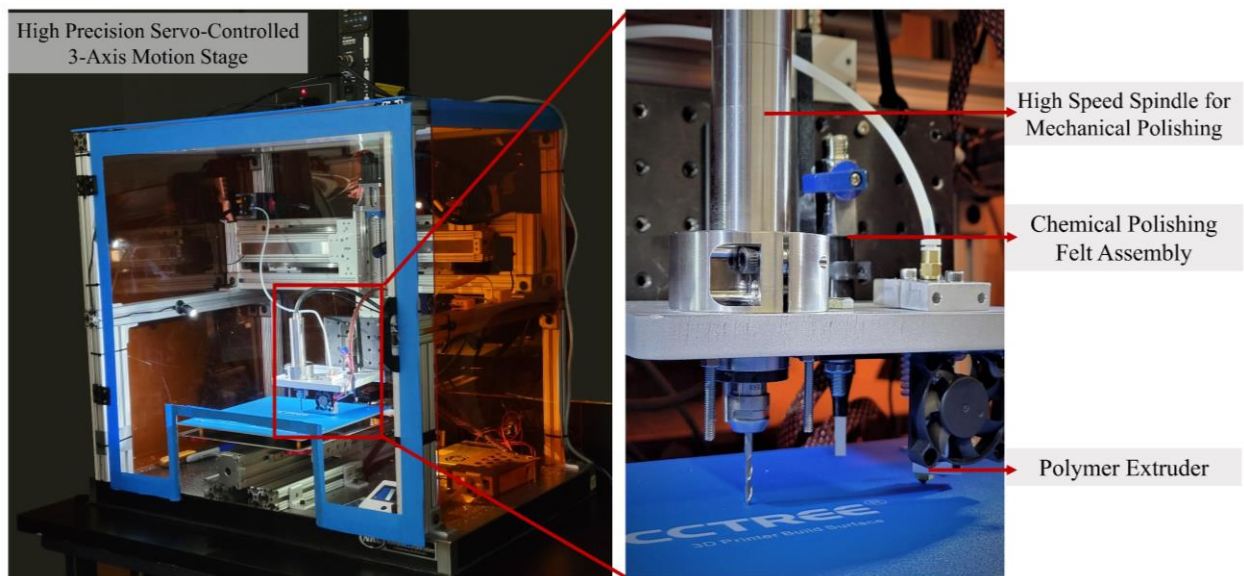


**Figure 1:** Custom-built setup with high precision 3-axis motion control stage, high-speed spindle for mechanical polishing, and a chemical polishing felt assembly.

For this study, specimens were printed in 30% (mass fraction) short glass fiber reinforced nylon-6 composite (Owens Corning, USA) using the FFF technique. The printing temperature was 245°C, and the heated platform temperature was 80°C. Manufacturing was done in an acrylic enclosure to maintain uniform temperature and prevent material warping. Cuboidal and cylindrical test specimens were produced to test polishing in straight-walled and curved surfaces. The dimensions are listed in Table 1. To make a direct comparison, the first 7 mm of the sample was left unpolished.

**Table 1.** Dimensional parameters for different specimen geometries.

<i>Parameter</i>	<i>Cuboid</i>	<i>Cylinder</i>
<i>Final desired X-Y dimension</i>	20 mm	20 mm
<i>Total height</i>	12 mm	12 mm
<i>Printed layer height</i>	0.2 mm	0.2 mm
<i>Polished height</i>	5 mm (25 layers)	5 mm (25 layers)
<i>Number of layers polished in 1 pass</i>	5	5

## 2.2 Polishing Control Strategy

Individual and combined mechanical and chemical polishing were performed utilizing an automated approach. Custom G-codes (Simply3D, USA) were generated by varying the polishing parameters according to the design of experiment. Cuboidal and cylindrical samples were polished along their outer periphery while the top and bottom surfaces were left as printed.

To automate the process, the part is manufactured using a two-step scheme [16]. This process employs a pseudo part at a distance from the primary printed part. The pseudo part is the outer shell of the primary print with modified dimensions. As shown in Fig. 2 (a), the tool offsets (distance between nozzle and the respective polishing tools) are applied to polish the primary part when the pseudo part is being printed. After a designated set of layers is polished, the printing continues on top of the partially polished primary part, and the cycle repeats itself.

As shown in Fig. 2 (b), to reach the desired final dimension compensating for the tool radius and the depth of polishing, the primary part is first printed at a larger dimension and then polished. For example, in the case of mechanical polishing for a desired final dimension of 20 mm, the primary part was designed to be 21 mm (i.e., 20 mm plus 2 two depths of cut of 0.5 mm) while the pseudo part was 23.18 mm (i.e., 20 mm plus a tool diameter). Similarly, for chemical polishing, the primary part was designed to be 20.2 mm (for a maximum pressing depth = 0.1 mm), while the pseudo part was 24.95 mm with a tool diameter of 4.95 mm.

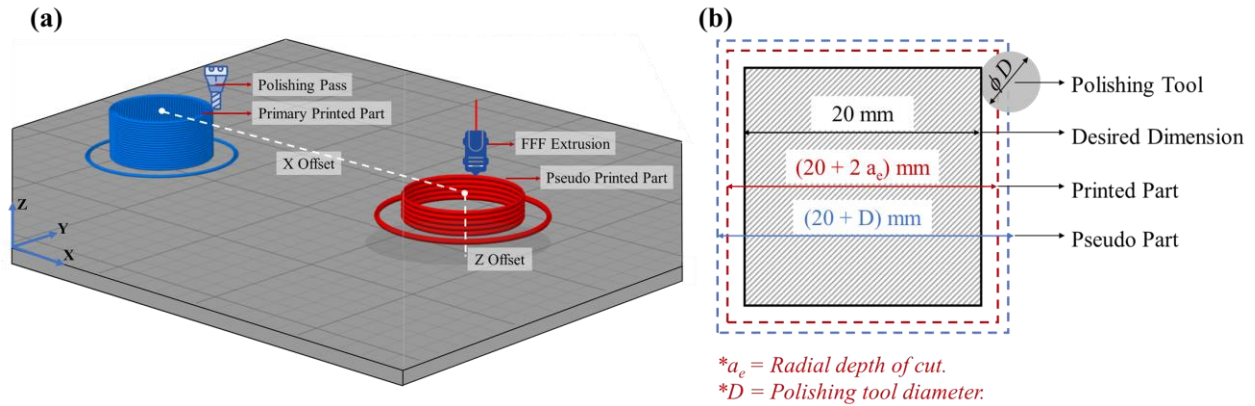


**Figure 2.** In-situ polishing strategy (a) polishing of primary part when pseudo part is being printed; (b) Tool radius and radial depth of cut compensation in the design process.

### 2.3 Parameters for Design of Experiment

In mechanical polishing, the cutting parameters should be meticulously selected as they directly affect the cutting forces, affecting the surface roughness. The chip load is the theoretical length of material fed into each cutting edge as it moves through the work material. As the chip load increases, it requires more force to shear the material being cut. Suppose the cutting forces were high while machining, the printed part adhered to the print platform may get disturbed, which may be detrimental to the surface finish. The chip load, therefore, was maintained below 0.05 mm. Also, to hold the workpiece material on the heated platform, down milling was performed. In down milling, cutting forces are directed downwards, thus pressing the workpiece rather than lifting it.

The design of experiment for mechanical polishing, as shown in Table 2, consisted of two levels of each spindle speed and the feed rate. The dependent variable is the surface roughness of the produced part.

**Table 2.** Design of experiment for mechanical polishing.

	<i>Case 1</i>	<i>Case 2</i>	<i>Case 3</i>	<i>Case 4</i>
<i>Spindle Speed (rpm)</i>	20000	20000	30000	30000
<i>Feed Rate (mm/min)</i>	800	1200	800	1200
<i>Chip load (mm)</i>	0.013	0.02	0.009	0.013

In chemical polishing, the material erosion rate depends on the concentration of the chemical solvent and the deposition rate. The chemical deposition rate is controlled by the chemical flow rate and the speed of polishing. In this experiment, the flow rate was kept constant while the speed of polishing was varied. Moreover, the radial force that the polishing felt applies on the printed part is defined by the pressing depth (directly proportional relation) [17]. Two pressing depths and polishing speeds were selected for comparison, as shown in Table 3.

**Table 3.** Design of experiment for chemical polishing.

	<i>Case 5</i>	<i>Case 6</i>	<i>Case 7</i>	<i>Case 8</i>
<i>Pressing Depth (mm)</i>	0.05	0.05	0.10	0.10
<i>Feed Rate (mm/min)</i>	600	800	600	800

In addition, optimum parameters from individual mechanical and chemical polishing were used to design a combined polishing strategy to investigate its performance compared to the individual polishing techniques. In this approach, mechanical polishing was performed first, which was followed by chemical polishing. Mechanical polishing acts as bulk material removal process and hence preceded chemical polishing, which can be characterized as finishing.

#### *2.4 Surface Roughness Characterization and Optical Measurements*

The manufactured samples were examined in macro and micro scales. The macro-scale analysis was conducted to assess the dimensional accuracy using Mitutoyo PH A41-profile projector (Kanagawa, Japan). The surface topography was analyzed for micro-scale analysis using Bruker ALICONA Infinite Vision (Raaba, Austria) on an area of  $2 \times 2 \text{ mm}^2$  using a 0.8 mm Gaussian filter (ISO-4288-1996). The Ra value was measured along and perpendicular to the feed direction for all polished faces. Both methods are based on non-contact measurement, suitable for polymer composites.

### **3. Result and Discussion**

Surface measurement results for mechanical, chemical, and combined polishing are presented in the following three sections.

#### *3.1 Surfaces after Mechanical Polishing*

The surface topography of the GFRP composites manufactured using FFF 3D printing is much different from the topography of the ones made through hand layup. The surface texture arises not only because of the abrasive nature of the material but also from the stair-stepping effect attributed to the layered printing. As shown in Fig. 3, the unpolished region of the part displays noticeable layering lines with fibers protruding out of the outer periphery. The average surface roughness (Ra) was measured across the four faces against the layering lines of each sample. It was computed to be  $22.52 \text{ }\mu\text{m}$  for cuboid and  $27.27 \text{ }\mu\text{m}$  for cylindrical samples.

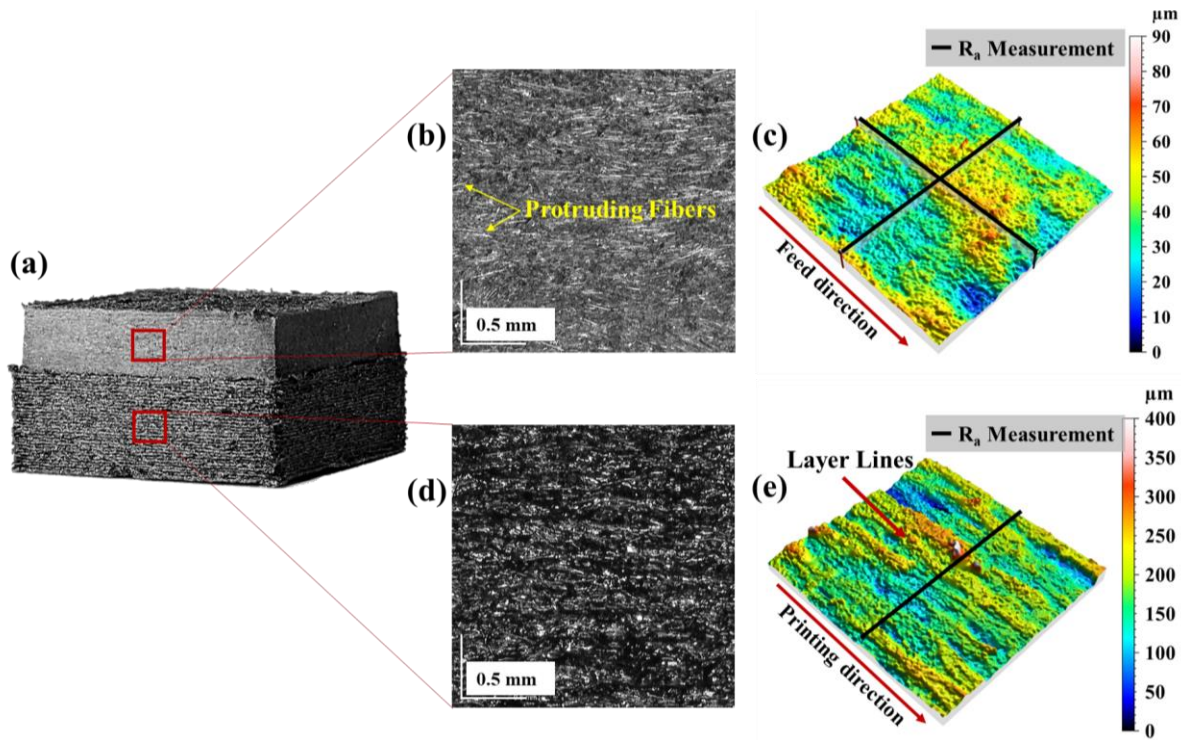


**Figure 3.** Mechanical polishing (a) cuboidal sample with unpolished and polished faces; (b) microscopic image of the polished face; (c) surface topography of the polished face; (d) microscopic image of the unpolished face; (e) surface topography of the unpolished face.

Generally, during milling of polymer composites, the fibers are exposed to shear stresses, inducing fiber failure at the cutting surface in the form of brittle fracture across the fiber, fiber pull-out and fiber-matrix debonding (by tensile fracture). This results in an overall smooth finish. After mechanical polishing at a depth of cut of 0.5 mm, the layer lines were eliminated, demonstrating a visibly smooth surface across all samples. Compared to the unpolished faces, mechanically polished faces in cuboid samples had sharper corners. However, both cuboidal and cylindrical specimens displayed exposed fibers protruding out of the machined surface, as shown in Fig. 3. This is also a common phenomenon in FPRs machining.

Fig. 4 shows the effect of polishing parameters on the average surface roughness ( $R_a$ ) for cuboid and cylindrical samples. To judge the impact of polishing,  $R_a$  was measured alongside feed and perpendicular to the feed direction (across the layer lines). A total of four measurements were made for each sample across four different faces. Further, analysis is discussed below:

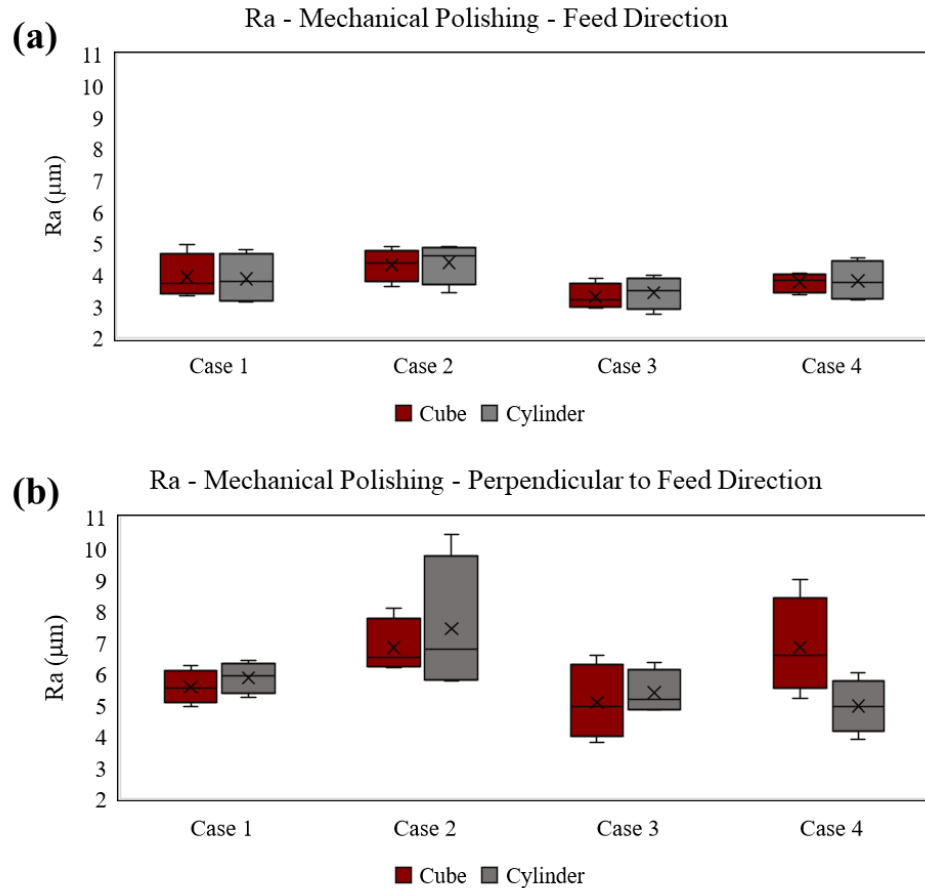


**Figure 4:** Mechanical polishing- variation of Ra with spindle speed and feed rate; (a) Ra measured along feed direction; (b) Ra measured perpendicular to feed direction.

- Paired T-test reveals no significant difference in the surface roughness of cuboidal and cylindrical samples for the same polishing parameters (p-value = 0.57 at 95% significance level). This indicates that mechanical polishing provides similar results irrespective of the geometry of the workpiece sample.
- After mechanical polishing, a significant difference exists in the Ra measured alongside feed and perpendicular to the feed direction for both the geometries (p-value cuboid = 0.01, p-value cylinder = 0.03 at 95% significance level). The surface roughness measured perpendicular to the feed direction is higher, suggesting that mechanical polishing is more effective in the feed direction.
- Further from Fig. 4, it can be inferred that the value of Ra increases with the feed rate and decreases with the spindle speed irrespective of the measurement direction. The best results were obtained for the polishing parameters of Case 3, which corresponded to the lowest chip load. Case 3 showed an 85.3% reduction for cuboid and an 85.45% reduction for cylindrical geometries compared to the unpolished region.
- Despite the smallest chip load (0.009 mm) with a theoretical roughness of 0.129 μm, the actual roughness is in twice the orders of magnitude larger. This indicates the limitations of roughness reduction by milling on FPRs.

### 3.2 Surfaces after Chemical Polishing

As shown in the microscopic images of Fig. 5, the chemically polished face exhibits an overall smooth surface finish, and the layer lines were eliminated. Unlike mechanical polishing, after chemical polishing, the fibers were encapsulated in the eroded polymer giving it a more uniform appearance. However, material accumulation in the form of surface beads was visible, which may negatively affect the surface finish.

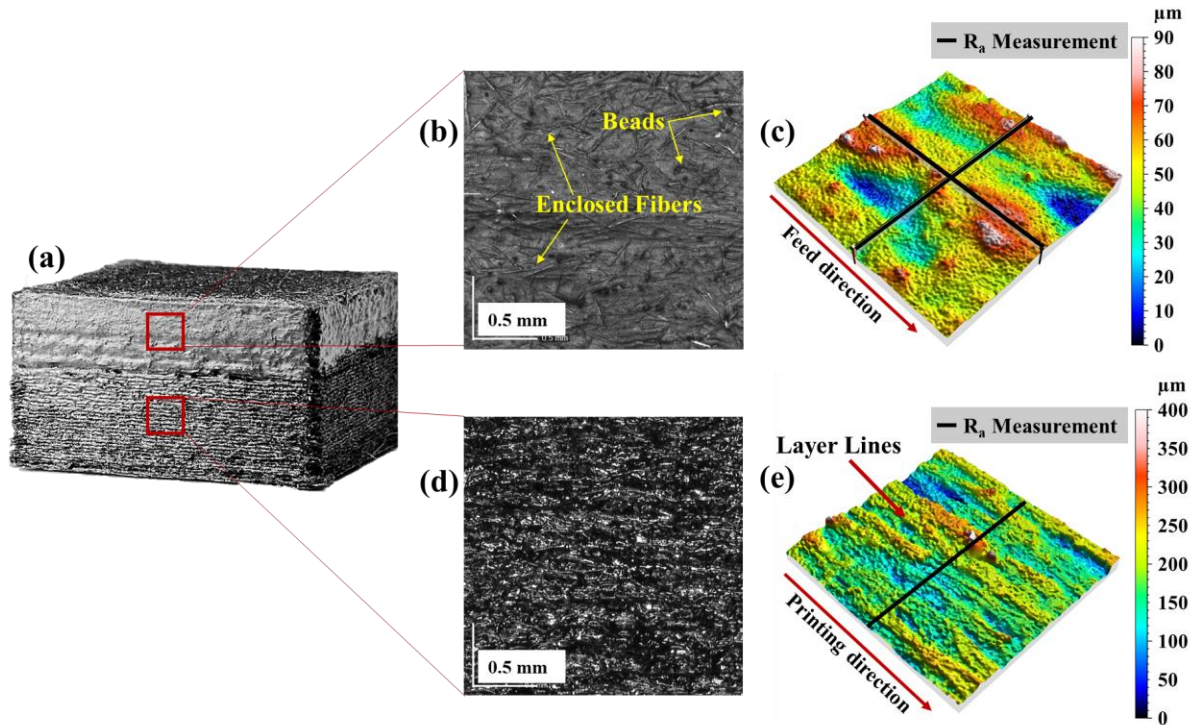


**Figure 5.** Chemical polishing (a) cuboidal sample with unpolished and polished faces; (b) microscopic image of the polished face; (c) surface topography of the polished face; (d) microscopic image of the unpolished face; (e) surface topography of the unpolished face.

Fig. 6 shows the effect of polishing parameters on the average surface roughness ( $R_a$ ) for cuboid and cylindrical samples. Polishing trials were conducted at pressing depths of 0.05 and 0.10 mm, and feed rates of 600 and 800 mm/min. Further, analysis is discussed below:

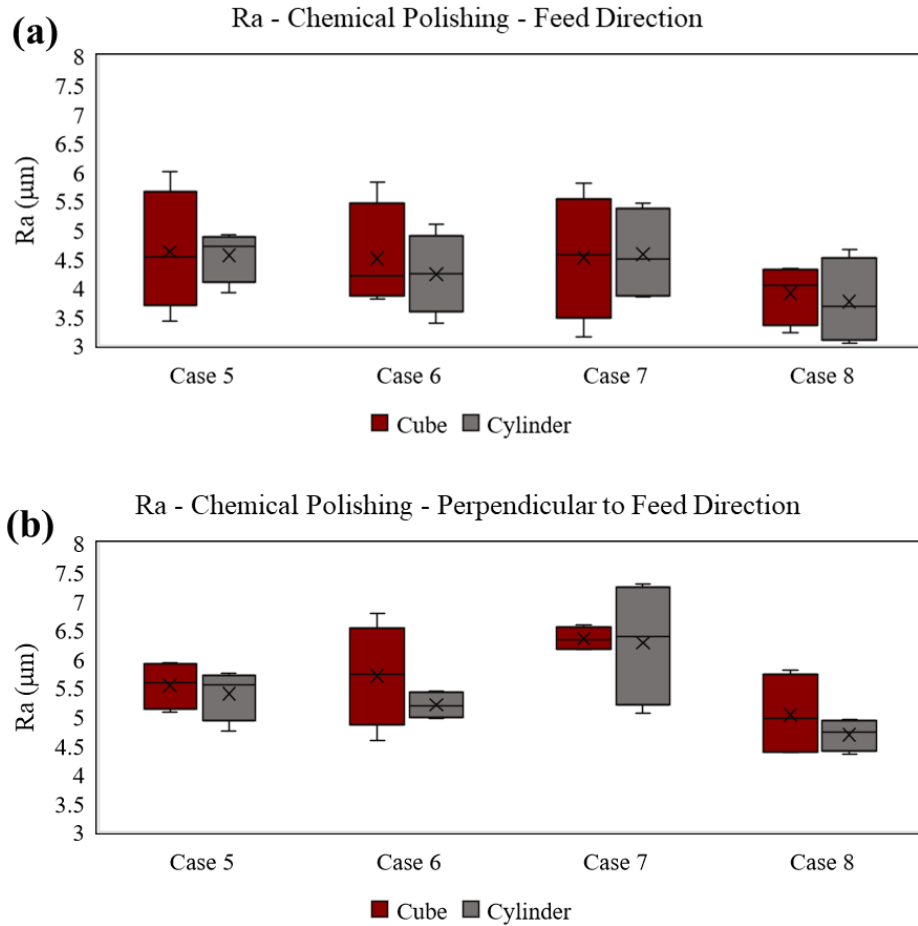


**Figure 6:** Chemical Polishing- variation of Ra with pressing depths and polishing speed; (a) Ra measured along feed direction; (b) Ra measured perpendicular to feed direction.

- Paired T-test reveals no significant difference in the surface roughness of cuboidal and cylindrical samples for the same polishing parameters (p-value = 0.59 at 95% significance level). This indicates that chemical polishing provides similar results irrespective of the geometry of the workpiece sample.
- After chemical polishing, no significant difference exists in the Ra measured alongside feed and perpendicular to the feed direction for both the geometries (p-value- cuboid = 0.09, p-value- cylinder = 0.08 at 95% significance level). This implies that unlike mechanical, chemical polishing is non-directional and effective in both directions.
- Further from Fig. 6, it can be inferred that minimum Ra was obtained for Case 8 (high pressing depth and high speed). Case 8 showed an 82.72% reduction for cuboid and an 86.24% reduction for cylindrical geometries compared to the unpolished region.
- On comparing the average results from Case 3 of mechanical polishing and Case 8 of chemical polishing, no significant difference exists in the Ra (p-value- cuboid = 0.98, p-value- cylinder = 0.27 at 95% significance level). This implies that chemical polishing reduces the Ra to a similar level to that of mechanical polishing at optimum parameters. However, it should be noted that their surface topographies are different.

### 3.3 Combined Mechanical and Chemical Polishing

From the previous sections on individual mechanical and chemical polishing, it can be observed that they have some limitations. Mechanical polishing is directional, while chemical polishing leads to the formation of surface beads. Therefore, this section examines a combined polishing approach and compares it to the previous results.

Optimum parameters obtained from the previous sections for individual mechanical and chemical polishing were used to design a combined polishing strategy to investigate its performance. The parts were manufactured using a three-step scheme- after printing a set of layers, mechanical polishing (spindle speed: 30000 rpm, feed rate: 800 mm/min) was conducted, which was followed by chemical polishing (pressing depth: 0.10 mm, feed rate: 800 mm/min).

As shown in Fig. 7, one part of each geometry was manufactured using the combined polishing method. The  $R_a$  was measured alongside feed and perpendicular to the feed direction (across the layer lines). The protruded fibers after machining were encapsulated in the eroded polymer. These encapsulated fibers were also shorter than those in the chemical-polishing-only cases. Further, the surface appeared to have fewer surface beads, meaning a more uniform erosion on a machined surface. Further analysis is discussed below:

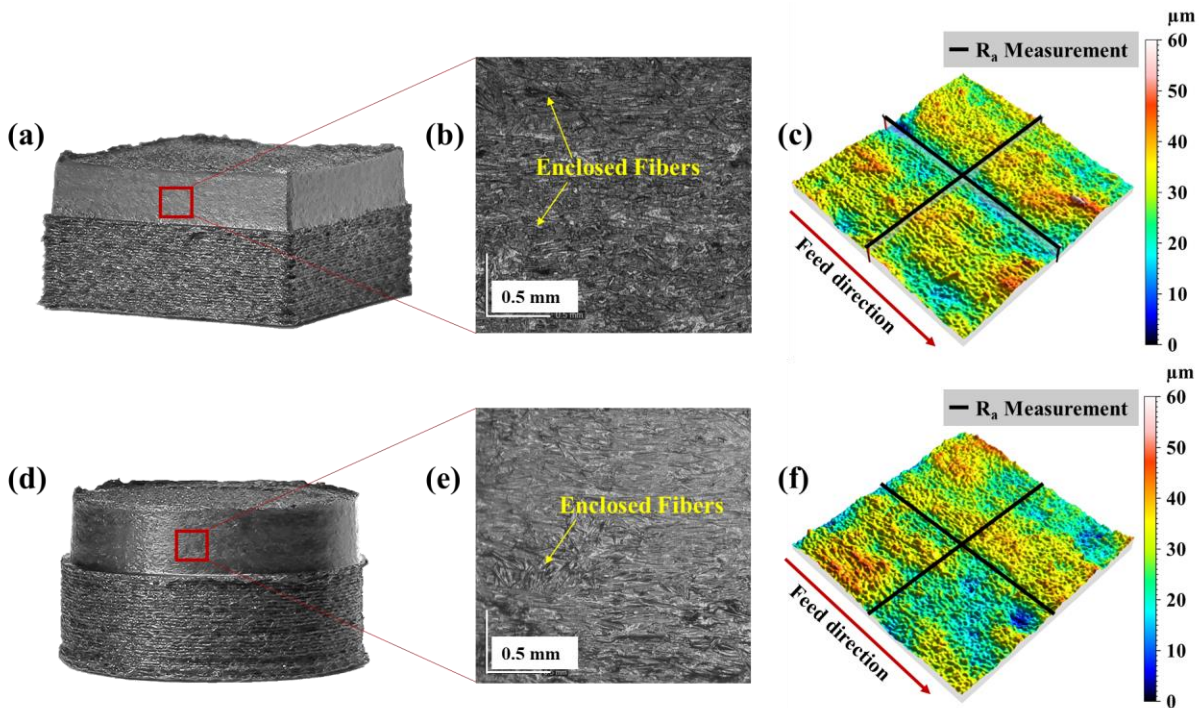


**Figure 7.** Combined polishing (a) cuboidal sample; (b) microscopic image of the polished face; (c) surface topography of the polished face; (d) cylindrical sample; (e) microscopic image of the polished face; (f) surface topography of the polished face.

- Paired T-test reveals no significant difference in the surface roughness of cuboidal and cylindrical samples for the same polishing parameters (p-value = 0.14 at 95% significance level). This indicates that the combined polishing technique provides similar results irrespective of the geometry of the workpiece sample.
- After combined polishing, no significant difference exists in the Ra measured alongside feed and perpendicular to the feed direction for both the geometries (p-value- cuboid = 0.07 p-value- cylinder = 0.10 at 95% significance level). This implies that combined polishing is non-directional and effective in both directions.
- Compared to the unpolished region, the cuboidal and cylindrical samples showed 89.8% and 90.1% reduction, respectively. The average Ra measured for cuboidal and cylindrical were 2.47  $\mu\text{m}$  and 2.93  $\mu\text{m}$ , respectively.
- As summarized in Fig. 8, combined polishing displayed maximum reduction in Ra irrespective of the measurement direction and part geometry.

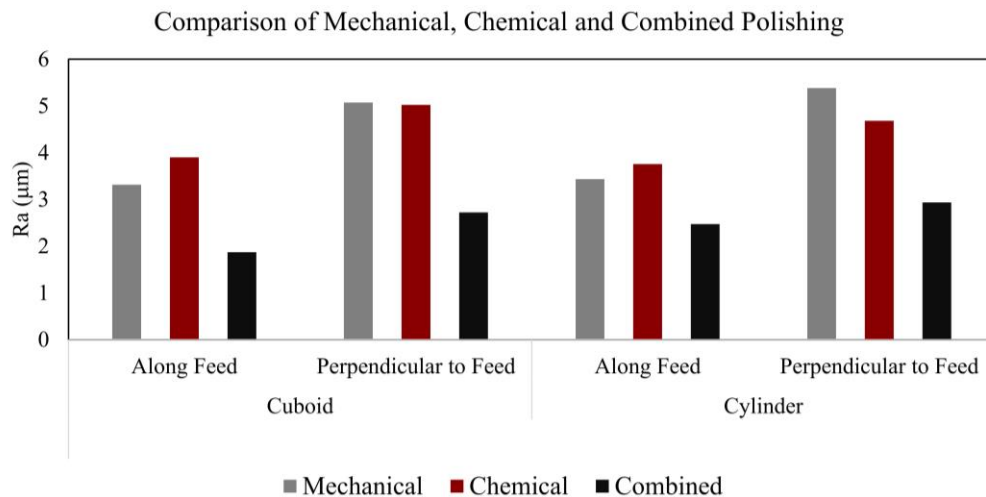


**Figure 8.** Summary- Effect of various polishing configurations on the surface roughness

### 3.4 Dimensional Accuracy

Apart from the microscopic analysis, macroscopic analysis was also performed to assess the dimensional accuracy of the polishing process for the samples polished with the most optimum parameters. The changes to the length and the width of the samples were measured for the two geometries. The results are summarized in Table 4. The dimensional accuracy for all cases has less than 1% error from the desired size. In fact, most of these dimensions are more accurate than a typical FFF 3D printing machine (0.1-0.5 mm). This suggests that the proposed polishing method can retain or even improve the dimensional accuracy.

**Table 4.** Measured dimensional error for different various polishing configurations.

	<i>Mechanical Polishing</i>		<i>Chemical Polishing</i>		<i>Combined Polishing</i>	
	<i>Cube</i>	<i>Cylinder</i>	<i>Cube</i>	<i>Cylinder</i>	<i>Cube</i>	<i>Cylinder</i>
<i>Designed Dimensions</i>	<i>Length 20 mm, Width 20 mm</i>					
<i>Measured Length (mm)</i>	20.12	20.09	20.02	20.04	20.14	20.14
<i>Measured Width (mm)</i>	20.07	20.07	20.03	20.11	20.01	20.01
<b><i>Length Error %</i></b>	<b>-0.6</b>	<b>-0.45</b>	<b>-0.1</b>	<b>-0.2</b>	<b>-0.7</b>	<b>-0.7</b>
<b><i>Width Error %</i></b>	<b>-0.35</b>	<b>-0.35</b>	<b>-0.15</b>	<b>-0.55</b>	<b>-0.05</b>	<b>-0.05</b>

#### 4. Conclusion

This parametric study examined an in-process polishing technique to enhance the surface finish of fiber-reinforced polymer parts manufactured through the FFF 3D printing technique. Experiments were conducted on a custom-developed 3-axis hybrid manufacturing setup with the capabilities of performing in-situ surface polishing. First, individual mechanical and chemical polishing was conducted, and the average surface roughness was measured for different polishing parameters and geometries. In addition, optimum parameters from individual polishing techniques were selected to design a combined polishing approach.

The results found that the employed polishing method plays a vital role in determining the average surface roughness. Both individual mechanical and chemical polishing leads to more than an 80% reduction in the Ra compared to the unpolished face. However, unlike chemical polishing, mechanically polished surfaces were found to be directional. Further, at optimum parameters derived from the individual polishing schemes, combined polishing outperformed them with more than a 90% reduction in Ra of the unpolished face. Also, no directionality was observed in the case of combined polishing.

Despite the apparent advantages of in-process polishing on GFPRs, many technical challenges remain and determine the future scope of this research. First, this study was based on glass fibers; it will be interesting to investigate the polishing behavior of other fiber materials or delicate mesh geometries. In the case of delicate mesh geometries, while conducting chemical polishing, the lack of radial force can be substituted with an increased solvent flowrate achieving a similar level of material erosion. However, while conducting mechanical polishing, reducing the depth of cut and chip load (hence the cutting forces) might be advantageous. This will be similar to micro-milling. Secondly, a higher magnification analysis is required to examine the fiber failure mechanism post polishing. Most importantly, it is critical to determine the effects of surface polishing on the mechanical performance of these GFRP manufactured parts.

This conclusion leads to the necessity for future expansion and an in-depth investigation of the in-situ process on its material removal mechanism.

## References

- [1] Farshbaf Zinati, R., & Razfar, M. R. (2013). An investigation of the machinability of PA 6/nano-CaCO<sub>3</sub> composite. *The International Journal of Advanced Manufacturing Technology*, 68(9-12), 2489–2497. <https://doi.org/10.1007/s00170-013-4875-3>
- [2] Palanikumar, K., Karunamoorthy, L., & Karthikeyan, R. (2006). Assessment of factors influencing surface roughness on the machining of glass fiber-reinforced polymer composites. *Materials & Design*, 27(10), 862–871. <https://doi.org/10.1016/j.matdes.2005.03.011>
- [3] Hancock, S. G. (2006). Forming woven fabric reinforced composite materials for complex shaped components: informing manufacture with virtual prototyping. 0000 0001 3529 6372.
- [4] Ming Ming, I. W., Azmi, A. I., Chuan, L. C., & Mansor, A. F. (2017). Experimental study and empirical analyses of abrasive waterjet machining for hybrid carbon/glass fiber-reinforced composites for improved surface quality. *The International Journal of Advanced Manufacturing Technology*, 95(9-12), 3809–3822. <https://doi.org/10.1007/s00170-017-1465-9>
- [5] Kabir, S. M., Mathur, K., & Seyam, A.-F. M. (2020). The Road to Improved Fiber-Reinforced 3D Printing Technology. *Technologies*, 8(4), 51. <https://doi.org/10.3390/technologies8040051>
- [6] Nigam, A, & Tai, BL. "Investigation of In-Situ Surface Polishing for Fused Filament Fabrication." *Proceedings of the ASME 2020 15th International Manufacturing Science and Engineering Conference. Volume 1: Additive Manufacturing; Advanced Materials Manufacturing; Biomanufacturing; Life Cycle Engineering; Manufacturing Equipment and Automation.* Virtual, Online. September 3, 2020. V001T01A053. ASME. <https://doi.org/10.1115/MSEC2020-8445>
- [7] Parandoush, P., & Lin, D. (2017). A review on additive manufacturing of polymer-fiber composites. *Composite Structures*, 182, 36–53. <https://doi.org/10.1016/j.compstruct.2017.08.088>
- [8] Elkington, M., Bloom, D., Ward, C., Chatzimichali, A., & Potter, K. (2015). Hand layup: understanding the manual process. *Advanced Manufacturing: Polymer & Composites Science*. <https://doi.org/10.1179/2055035915y.0000000003>
- [9] Kuram, E. (2016). Micro-machinability of injection molded polyamide 6 polymer and glass-fiber reinforced polyamide 6 composite. *Composites Part B: Engineering*, 88, 85–100. <https://doi.org/10.1016/j.compositesb.2015.11.004>
- [10] Parandoush, P, Deines, T, Lin, D, Zhang, H, & Ye, C. "Mechanical Finishing of 3D Printed Continuous Carbon Fiber Reinforced Polymer Composites via CNC Machining." *Proceedings of the ASME 2019 14th International Manufacturing Science and Engineering Conference. Volume 1: Additive Manufacturing; Manufacturing Equipment and Systems; Bio and Sustainable Manufacturing.* Erie, Pennsylvania, USA. June 10–14, 2019. V001T01A003. ASME. <https://doi.org/10.1115/MSEC2019-2972>
- [11] Murphy, C., Byrne, G., & Gilchrist, M. D. (2002). The performance of coated tungsten carbide drills when machining carbon fibre-reinforced epoxy composite materials. *Proceedings of the*

Institution of Mechanical Engineers, Part B: Journal of Engineering Manufacture, 216(2), 143–152. <https://doi.org/10.1243/0954405021519735>

[12] Altin Karataş, M., & Gökkaya, H. (2018). A review on machinability of carbon fiber reinforced polymer (CFRP) and glass fiber reinforced polymer (GFRP) composite materials. *Defence Technology*, 14(4), 318–326. <https://doi.org/10.1016/j.dt.2018.02.001>

[13] Jayanth, N., Senthil, P., & Prakash, C. (2018). Effect of chemical treatment on tensile Prototyping, 13(3), 155–163. <https://doi.org/10.1080/17452759.2018.1449565>

[14] Neff, C., Trapuzzano, M., & Crane, N. B. (2018). Impact of vapor polishing on surface quality and mechanical properties of extruded ABS. *Rapid Prototyping Journal*, 24(2), 501–508. <https://doi.org/10.1108/rpj-03-2017-0039>

[15] Kuo, C.-C., Wang, C.-W., Lee, Y.-F., Liu, Y.-L., & Qiu, Q.-Y. (2016). A surface quality improvement apparatus for ABS parts fabricated by additive manufacturing. *The International Journal of Advanced Manufacturing Technology*, 89(1-4), 635–642. <https://doi.org/10.1007/s00170-016-9129-8>

[16] Nigam, A., & Tai, B. L. (2021). In-process chemical and mechanical polishing for fused filament fabrication: A feasibility study. *Manufacturing Letters*, 28, 59–62. <https://doi.org/10.1016/j.mfglet.2021.04.001>

[17] Takagishi, K., & Umezu, S. (2017). Development of the improving process for the 3d printed structure. *Scientific Reports*, 7(1). <https://doi.org/10.1038/srep39852>